Received: May 7, 2023. Revised: June 16, 2023. 630

International Journal of
Intelligent Engineering & Systems

http://www.inass.org/

# Repeated Clipping Filtering with Nonlinear Companding for PAPR Reduction in MIMO FBMC/OQAM System

**Ammar Boudjelkha[1]* Abdellatif Khelil[1] Hocine Merah[2]**

[1]*LGEERE Laboratory, Electrical Engineering Department, Faculty of Technology, Echahid Hamma Lakhdar University, El Oued, Algeria*
[2]*Semiconductors and Functional Materials Laboratory, Electronics Department, University Amar Telidji, Laghouat, 03000, Algeria*
* Corresponding author's Email: boudjeam@gmail.com

**Abstract:** Multi-carrier modulation (MCM) is one of the fundamental components of beyond 5G (B5G) and 6G that meets the many requirements of contemporary use cases. Filter bank multi-carrier with offset quadrature amplitude modulation (FBCM/OQAM) is one of the most promising modulation that offers many benefits to the next generation. However, like all MCM modulations, it shows a high peak signal in the time domain, which causes in-band (IB) and out-of-band (OOB) distortions in the amplifier output signal. The present paper suggests that an FBMC/OQAM system with multi-input multi-output (MIMO) employs a new hybridization that combines repeated clipping filtering (RCF) with several companding techniques, including A-Law, Mu-Law, tangente rooting (tanhR), logarithmic rooting (logR), cos and rooting companding (RTC). The combination of RCF and Mu-Law yields the best results of peak-to-average power ratio (PAPR) reduction and bit error rate (BER). The simulation results showed a significant decrease in PAPR, with a reduction of 68.54% compared to the original signal without the reduction technique.

**Keywords:** 5G, MIMO FBMC/OQAM, RCF, Nonlinear companding, Hybridization, HPA, PAPR, BER.

## 1. Introduction

The user requirements for enhanced mobile broadband (eMBB), massive machine-type communication (mMTC) and ultra-reliable low latency communication (uRLLC) are becoming increasingly stringent. These necessitate a high level of energy and spectrum efficiency [1,2]. Standard modulation named orthogonal frequency division multiplexing (OFDM), widely used in the wireless domain, suffers in spectral efficiency and energy efficiency following the use of cyclic prefix (CP), high sidelobes with high sensitivity to the carrier frequency offset (CFO) [3]. The FBMC/OQAM can overcome these constraints by employing a prototype filter that is well localized in time and frequency and operates efficiently in an environment with several users, high levels of interference and high mobility. The FBMC/OQAM is well-known, in the literature for its excellent spectrum efficiency multiple robustness against intercarrier interference (ICI) and intersymbol interference (ISI), multipath effects and CFO, among other things [4]. These advantages make FBMC an attractive candidate for future generations. However, like all MCM systems, FBMC/OQAM suffers from a high PAPR of the transmitted signal in the time domain. High PAPR is mainly due to the high amplitude peaks of the FBMC/OQAM signal, which are brought on by using the superposition of the modulated symbols on the subcarriers in the MCM scheme with a probability that these symbols have the same phase. These high amplitude peaks force the high-power amplifier (HPA) to operate outside the linear zone. Thus, the IB and OOB distortions degrade the BER performance [5-7]. In the literature, the researchers propose several PAPR reduction techniques as solutions to this challenge. They include clipping, companding, precoding, partial transmission sequence (PTS), tone reservation (TR), tone injection (TI), active constellation

extension (ACE) and selective mapping (SLM). The authors in [8] proposed the clipping technique, which is simple to implement and based on eliminating peaks higher than a predetermined threshold. Enhancing the BER and recovering the source signal, clipping technique requires a distortion correction algorithm. In order to further enhance the performance of FBMC/OQAM, hybridization of clipping with other techniques is suggested. [9] proposes an alternative based on clipping combined with non-linear companding techniques employing discrete fourier transform (DFT) spread with the polyphase network. The simulations produced good results in lowering the PAPR while maintaining acceptable BER performance. TR-DC in [10] is a hybridization based on the TR technique with an improved clipping; called deep clipping (DC). Taking advantage of the linearity of TR and the low complexity of DC, this method improves the performance of PAPR reduction and reduces complexity. In [11], the adaptive clipping (AC) technique allows adaptive adjustment of the clipping amplitude size. The ACE method based on the overlapping scale intelligent gradient projection (OSGP) program increases the convergence speed of the system. The combination of these two algorithms considerably improves the overall performance of the FBMC/OQAM system and ensures the trade-off between the PAPR, BER and computational complexity. In a visible light communication (VLC) based FBMC system, researchers suggest in [12] the clipping method with discrete cosine transform (DCT) precoding and Hadamard transform separately, then evaluate it with that of VLC-based OFDM. The VLC-based FBMC system performs better in terms of PAPR reduction and BER than the VLC-based OFDM system. [13] combines an improved bilayer partial transmit sequence (IBPTS) with iterative clipping and filtering (ICF) named (IBPTS-ICF) technique that uses the ICF to reduce distortion and the bilayer PTS to reduce complexity. This technique combines (PTS and ICF) to enhance performance by minimizing PAPR, complexity and distortions.

Companding techniques are another form for reducing PAPR, which have low computational complexity, excellent BER and flexibility. It applies the inverse of companding in the receiver. There are several companding methods, including the tanhR, cos, RTC, absolute exponential companding (AEXP), logR, Mu-law and A-law companding. The companding techniques used by several researchers, such as the authors of [14] suggest a scheme based on absolute exponential companding (AEXC) in order to lower the PAPR. Simulations show that this method effectively reduces the PAPR by compressing signal peaks and expanding weak signals. The RTC technique forms the base for the method suggested in [15]. It provides higher PAPR reduction performance with better BER results. The authors of [16] suggest a technique based on linear companding. This method demonstrates an improved PAPR reduction, excellent BER performance and a spectrum with fewer sidelobes than the nonlinear companding method Mu-Law through numerical results. An FBMC/OQAM system is used in [17, 18] to apply various companding techniques. Mu-Law presented the highest PAPR reduction, best BER and good power spectral density (PSD) results. [19] presents a comparison of the two methods, A-Law and Mu-Law. The A-Law companding technique is the best for BER. However, numerical experiments showed that A-Law is only marginally superior in PAPR reduction. The analysis of the enhanced logarithmic rooting companding (LRC) in [20] shows that its performances are superior to other nonlinear companding approaches. By selecting the optimal LRC parameters, the authors achieved a compromise between the best outcomes in reducing PAPR and BER. The authors suggest the weibull companding (WC) in [21] which is new non-linear companding that consists of transforming the amplitude of the FBMC signal into a Weibull transformation, where the simulation results show the effective trade-off between BER and PAPR reduction. Using the companding with other techniques to further improve the PAPR and BER performances is also proposed in the literature. The authors of [22] presented the combination of the trellis-based selective mapping (TSLM) and A-Law companding and compared the results with the individual performance of TSLM and A-Law. Then, by striking a compromise between the various PAPR indicators, computational complexity and BER, the suggested scheme can enhance the PAPR more than the TSLM for the same computational complexity and improve the BER than the A-Law for the same PAPR. tone injection (TI) and Mu-Law perform more effectively jointly than they do independently to enhance results with the same number of iterations in [23]. The Mu-Law, non-orthogonal multi-access (NOMA) and asymmetrically-clipped optical (ACO) techniques are combined, according to researchers in [24], for the FBMC/OQAM system on a VLC channel. The simulations show a decrease in PAPR, as well as a notable increase in throughput and a decrease in unserved users. The paper [25] presented the linear companding with iterative filtering. This

combination successfully lowers PAPR and enhances BER outcomes, with using iteration to effectively minimize OOB distortions produced by companding. The efficiency of this method compared to companding techniques is supported by the numerical results of the simulation.

MIMO technology greatly increases communication coverage, throughput, and reliability by utilizing several antennas for transmission and reception [26]. There are numerous solutions in the literature to the MIMO FBMC/OQAM system's high PAPR problem. The authors of [27] presented the combination of the alamouti-coded FBMC scheme without ICI and the FBMC low PAPR scheme based on the DFT spread. The numerical results are greatly improved in both PAPR reduction and BER performance. In [28], the simulation results of the combination of A-Law and Mu-Law methods with the walsh-hadamard transform (WHT) precoding method in the MIMO FBMC/OQAM system based on space frequency block coding (STBC) confirm that the A-Law combined with WHT has the best PAPR and BER compared to WHT with the Mu-Law combination. Additionally, both the A-Law and Mu-Law techniques have low implementation complexity. The extended preamble structure, which the researchers suggest in [29], uses the symmetry pattern to cancel interference and provides a low PAPR with enhanced BER and mean square error (MSE). Permutation inversion (PI), which lowers PAPR and computational complexity, is suggested in [30] for MIMO OFDM/OQAM systems. The attenuating quadrature amplitude modulation symbols (AQAMS) scheme in the MIMO FBMC/OQAM system does not need side information (SI) as presented in [31]. It employs a simple multiplier between the sequence of QAM complex symbols and the attenuation coefficient; an improvement in BER and PAPR is shown in the simulation. The researchers suggest in [32] the successive addition subtraction (SAS) method with WHT to reduce the PAPR of the MIMO FBMC/OQAM scheme. It can successfully improve the PAPR reduction and the BER performance.

Techniques for PAPR reduction are evaluated in terms of PAPR reduction, BER, transmission data rate and computational complexity. Some are particularly good at reducing the PAPR while maintaining a good BER, but they also require the transmission of side information (SI) to reception, which greatly increases the computational complexity and reduces throughput, as in the cases of PTS, SLM, ACE and TR. Other methods have the advantage that they are efficient at lowering the PAPR, simple to implement and have minimal computational complexity, but these benefits come at the cost of distortion of the transmitted signal, such as clipping. Another technique for reducing PAPR is known as companding, which has a modest rate of PAPR reduction but is easy to implement, has low computational complexity, and has a good BER.

Combining two or three of these methods—typically applied in cascade—allows for greater PAPR reduction while also gaining the benefits of each method combined.

As mentioned in the state of the art, the techniques combined with the RCF are methods with a high level of PAPR reduction and good performance in BER, but their computational complexity is remarkably high and they require an SI to transmit it on reception, which significantly reduces the transmission rate. Moreover, not using MIMO technology in the FBMC/OQAM scheme is another weak point in these studies.

To my knowledge, this is the first study to suggest this hybridization based on combining the RCF technique with the companding technique to reduce the PAPR of the MIMO FBMC/OQAM system. Clipping is particularly effective at lowering PAPR but suffers from high distortion. While filtering removes the OOB distortions caused by clipping, it also suffers from spectral regrowth, which causes new peaks to be repelled again and PAPR to be increased. RCF ensures the removal of OOB distortions caused by clipping and IB peaks caused by filtering. Companding is another technique that shows good BER performance but a very modest PAPR reduction. It cascades the RCF, allowing for a further reduction in the PAPR with less complexity. In order to reduce distortion and consequently enhance BER, various adjustments can be beneficial. The companding schemes proposed in this study include A-Law, Mu-Law, TanhR, LogR, RTC, and cos. Combining these methods ensures effective PAPR reduction using the clipping method and effective BER using the companding method. The recommended method is a potent variation that can be employed in future generations because it also guarantees simplicity in implementation, has a low level of computation complexity, and does not require the transfer of any SI.

The main contributions of this article are the combination of the RCF and the companding techniques, the implementation of a multi-antenna scenario (MIMO) with 2x2 antennas instead of a single antenna scheme (SISO) in the FBMC/OQAM system, and the use of two low-complexity techniques like RCF and companding to keep more computational complexity down.

The rest of this work is organized as follows: section 2 presents the theoretical analysis of FBMC/OQAM modulation. Section 3 expands this analysis to include MIMO technology. Section 4 provides a mathematical description of the PAPR and CCDF. Section 5 discusses PAPR reduction techniques, whereas section 6 explains the RCF in combination with the companding algorithm. Section 7 details the numerical results of the simulation of the proposed method. Finally, the conclusion is displayed.

## 2. FBMC system

The FBMC/OQAM system uses the synthesis and analysis of filter banks in the transmitter and receiver, respectively, with *N* subcarriers and *1/N* subcarrier spacing. The FBMC modulation is only orthogonal in the real part. The complex symbols consist of two fields, real and imaginary domains. Recovering the real value $a_{m.n}$ by extracting real and imaginary parts of the QAM symbol. Then transmit the real-valued symbols $a_{m,n}$ at an interval of *T/2* [33, 29]. The transmitted signal is written as follows [34]:

$$x(t) = \sum_{m=0}^{N-1} \sum_{n=-\infty}^{+\infty} a_{m.n} h_{m.n}(t) \quad (1)$$

$a_{m.n}$ represents the real of the OQAM symbol and $h_{m.n}(t)$ indicates the prototype filter. $m$ and $n$ represent successively the subscriber index and the symbol time index.

$$h_{m.n}(t) = h(t - n\tau) e^{i2\pi m F_0 t} e^{j\emptyset_{m.n}} \quad (2)$$

$h(t)$ represents a symmetric real-valued of pulse filter, $\tau$ is the time shift between the two constituent parts of the FBMC/OQAM symbol: the real and imaginary parts. $T$ is the symbol duration and $F=1/T=1/2\tau$ which designates the subcarrier spacing and $\emptyset_{m,n}$ indicates the phase term.

Knowing that the functions of the filter $h_{m.n}(t)$ are orthogonal in the real part with:

$$\Re\{\langle h_{m.n} | h_{m_0.n_0} \rangle\} = \Re\{\sum_{t=-\infty}^{+\infty} h_{m.n}(t) h^*_{m_0.n_0}(t)\} = \delta_{m.m_0} \delta_{n.n_0} \quad (3)$$

Here $\Re(.)$ defines the real part of a complex number symbol and $\delta$ is the Kronecker delta function whose:

$$\delta_{m,m_0} = \begin{cases} 1, & if\ m = m_0 \\ 0, & if\ m \neq m_0 \end{cases} \quad (4)$$

At the output of the filter bank, the imaginary intercarrier interference is present even in the case of a channel without distortion.

On receiving, the reverse process is used to recover the original signal.

$$r(t) = \sum_{m=0}^{N-1} \sum_{n=-\infty}^{+\infty} a_{m.n} h_{m.n}(t)\, U_{m.n}(t) + w(t) \quad (5)$$

$w(t)$ represents the additive white Gaussian noise (AWGN). While $U_{m.n}(t)$ indicates the channel complex response at time domain.

$$U_{m.n}(t) = \int_0^{\tau_{max}} h(t.\tau) e^{-2j\pi F_0 \tau} d\tau \quad (6)$$

Where $h(t.\tau)$ represents channel impulse response.

The output symbols of the analysis filter bank (AFB) are affected by a pure imaginary interference called Intrinsic Interference. By projecting the received signal *r(t)* on the corresponding receive subchannel filter $h^*(t)$, the demodulated signal $y_{m_0.n_0}$ ,at subcarrier $(m_0)$ and multicarrier $(n_0)$, can be obtained as [33, 29]:

$$y_{m_0,n_0} = \langle r | h_{m_0.n_0} \rangle \quad (7)$$

$$y_{m_0.n_0} = U_{m_0.n_0} a_{m_0.n_0} + \sum_{(m.n)\neq(m_0.n_0)} U_{m.n} a_{m.n} \langle h \rangle_{m.n}^{m_0.n_0} + w_{m_0.n_0} \quad (8)$$

Where $U_{m_0.n_0}$ denotes the channel frequency response, from the receiver to the transmitter antennas, at subcarrier $(m_0)$ and multicarrier $(n_0)$, $w_{m_0.n_0}$ represents the additive white gaussian noise (AWGN) and the intrinsic interference is represented as:

$$I_{m_0.n_0} = \sum_{(m.n)\neq(m_0.n_0)} U_{m.n} a_{m.n} \langle h \rangle_{m.n}^{m_0.n_0} \quad (9)$$

In addition, $\langle h \rangle_{m.n}^{m_0.n_0}$ denotes the interference weight, which can be written in the following form [29, 35]:

$$\langle h \rangle_{m.n}^{m_0.n_0} = -j \langle h_{m.n} | h_{m_0.n_0} \rangle = \int h_{m.n}(t) h^*_{m_0.n_0}(t)\, dt \quad (10)$$

Where $\langle h_{m.n} | h_{m_0.n_0} \rangle$ represents the pure imaginary term for $(m.n) \neq (m_0.n_0)$, Knowing the filter prototype $h_{m.n}$ is well localized in time and frequency. Supposing the intrinsic interference is caused by the point's first-order neighbors. $\Omega^*$

represents the neighborhood and $(m.n)$ can take the values of $\Omega^*$ [35].

$$\Omega^* = \{(m_0.n_0 \pm 1), (m_0 \pm 1.n_0), (m_0 \pm 1.n_0 \pm 1)\} \quad (11)$$

Assuming that the frequency response of the channel is invariant in the FBMC system, we will therefore have:

$$y_{m_0.n_0} = U_{m_0.n_0} a_{m_0.n_0} + U_{m_0.n_0} \sum_{(m.n)\in\Omega^*} a_{m.n} \langle h \rangle_{m.n}^{m_0.n_0} + w_{m_0.n_0} \quad (12)$$

$$y_{m_0.n_0} = U_{m_0.n_0}\left(a_{m_0.n_0} + \sum_{(m.n)\in\Omega^*} a_{m.n} \langle h \rangle_{m.n}^{m_0.n_0}\right) + w_{m_0.n_0} \quad (13)$$

Consequently, $y_{m_0.n_0}$ can be expressed as the following:

$$y_{m_0.n_0} = U_{m_0.n_0}\left(a_{m_0.n_0} + jz_{m_0.n_0}\right) + w_{m_0.n_0} \quad (14)$$

Where $jz_{m_0.n_0}$ represents the FBMC system's orthogonal imaginary interference.

$$jz_{m_0.n_0} = \sum_{(m.n)\in\Omega^*} a_{m.n} \langle h \rangle_{m.n}^{m_0.n_0} \quad (15)$$

And:

$$c_{m_0.n_0} = a_{m_0.n_0} + jz_{m_0.n_0} \quad (16)$$

To allow the receiver to recover the sent signal, it is necessary to take the real part of the demodulated signal and drop the imaginary one.

$$a_{m_0.n_0} = \Re\{c_{m_0.n_0}\} \quad (17)$$

## 3. MIMO FBMC/OQAM system

The proposed MIMO FBMC / OQAM system is equipped with $D_t$ transmitting antennas and $D_r$ receiving antennas as presented in Fig. 1.

The received signal for each receives antenna is written as [3, 36, 37]:

$$y_{m_0.n_0}^{D_r} = U_{m_0.n_0}^{D_r.D_t}\left(a_{m_0.n_0}^{D_t} + jz_{m_0.n_0}^{D_t}\right) + w_{m_0.n_0}^{D_r} \quad (18)$$

Where $U_{m_0.n_0}^{D_r.D_t}$ denotes the channel complex response between the $D_t\,th$ transmit antenna and the $D_r\,th$ receive antenna at frequency $m_0$ and time instant $n_0$. $a_{m_0.n_0}^{D_t}$ is the real OQAM symbol at the $D_t\,th$ transmit antenna. $z_{m_0.n_0}^{D_t}$ corresponds to the imaginary interference part and the noise created by the transmitter antenna is presented by $w_{m_0.n_0}^{D_r}$. Eq. (19) writes the MIMO-FBMC/OQAM signal as:

$$y_{m_0.n_0} = U_{m_0.n_0} c_{m_0.n_0} + w_{m_0.n_0} \quad (19)$$

Which can be represented with the matrix form as:

$$\begin{pmatrix} y_{m_0.n_0}^1 \\ \vdots \\ y_{m_0.n_0}^{D_r} \end{pmatrix} = \begin{pmatrix} U_{m_0.n_0}^{1.1} & \cdots & U_{m_0.n_0}^{1.D_t} \\ \vdots & \ddots & \vdots \\ U_{m_0.n_0}^{D_r.1} & \cdots & U_{m_0.n_0}^{D_r.D_t} \end{pmatrix} \begin{pmatrix} c_{m_0.n_0}^1 \\ \vdots \\ c_{m_0.n_0}^{D_t} \end{pmatrix} + \begin{pmatrix} w_{m_0.n_0}^1 \\ \vdots \\ w_{m_0.n_0}^{D_r} \end{pmatrix} \quad (20)$$

Where $U_{m_0.n_0}$ is $(D_t\ x\ D_r)$,

## 4. PAPR and CCDF

The PAPR of a signal $x(n)$ can be defined as the value of the ratio of the peak value to the average value [31]:

$$PAPR_{x(n)} = \frac{\underset{iNL\le n\le (i+1)NL-1}{max} \{|x(n)|^2\}}{E\{|x(n)|^2\}}, i\epsilon\mathbb{N} \quad (21)$$

Where $N$ is the number of subcarriers, $L$ is the oversampling factor and is denoted as: $E[.]$ is the expectation operation.

The cumulative distribution function ($CDF$) of the FBMC signals $x(n)$

$$CDF = Pr\{PAPR_{x(n)} < PAPR_0\} \quad (22)$$

The complementary cumulative distribution function ($CCDF$) shows the probability $Pr$ when $x(n)$'s PAPR reaches a $PAPR_0$ threshold.

$$CCDF = Pr\{PAPR_{x(n)} \ge PAPR_0\} \quad (23)$$

The FBMC/OQAM system with 2x2 antennas of the MIMO technique. Eq. (24) presents the PAPR as:

$$PAPR_{MIMO} = max\{PAPR_{x_1(n)}., PAPR_{x_2(n)}\} \quad (24)$$

Here $x_1(n)$ and $x_2(n)$ represented the signals to be transmitted by antenna 1 and 2.

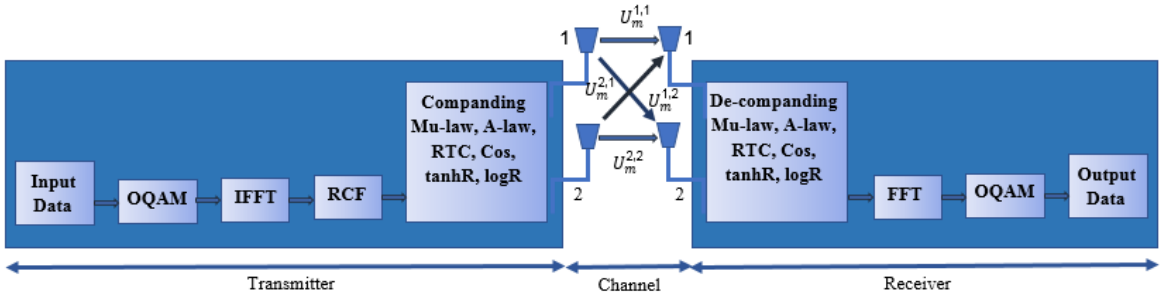


Figure. 1 MIMO FBMC/OQAM block diagram with the combination of RCF and companding techniques

## 5. PAPR reduction techniques

### 5.1 Repeated clipping and filtering (RCF)

In the literature, clipping is considered the simplest method among PAPR reduction techniques. It eliminates the component of the signal that exceeds a predefined threshold amplitude, Amax. It is written as follows [38, 39]:

$$x_c = \begin{cases} A_{max}, & if \;\; x > A_{max} \\ x, & if \;\; x \le A_{max} \end{cases} \quad (25)$$

Where $x$ is the input signal, $A_{max}$ is the predefined threshold amplitude.

After transforming the signal $x_c$ from the time domain to the frequency domain $X_c$, filtering after clipping removes all OOB distortion caused by clipping, which is presented as [40, 41]:

$$X_c' = \begin{cases} X_c, & if \;\; i\epsilon[0.,N-1] \\ 0, & other \end{cases} \quad (26)$$

Where $X_c$ represents $x$ in the frequency domain.

The filtering technique allows to regenerate of signal peaks and the RCF considerably eliminate the IB distortions with the eventual reproduction of the

signal peaks. This technique known as RCF, gives better results when compared to the clipping and filtering (CF) technique [42].

### 5.2 Companding techniques

The companding technique is one of the most basic PAPR reduction methods, with low computing complexity and excellent BER performance. At the transmitter, this technique transforms the high-amplitude signal into a uniformly distributed signal and the reverse process is done at the receiver to restore the original signal [38, 43]. The following is a summary of the many companding techniques.

#### 5.2.1. Mu-law companding

The Mu-law companding for the $x$ input signal is as follows [28, 44]:

$$F(x) = sgn(x)\frac{ln\,(1+Mu|x|}{ln\,(1+Mu)} \quad (27)$$

Where $Mu$ represents the control parameter of the level of companding applied to the signal. Therefore, Eq. (28) gives the de-companding form:

$$F^{-1}(r) = sgn(r)\frac{1}{Mu}((1+Mu)^{|r|}-1) \quad (28)$$

#### 5.2.2. A-companding

The Eq. (29) shows the A-law companding for the x input signal as [28,45]:

$$F(x) = sgn(x)\begin{cases} \frac{A|x|}{1+ln(A)}, & if \;\; |x| < \frac{|x|_{max)}}{A} \\ \frac{1+ln(A|x|)}{1+ln(A)}, & if \;\; |x| \ge \frac{|x|_{max)}}{A} \end{cases} \quad (29)$$

Where $A$ represents the companding parameter and $sgn(x)$ is a sign of the signal.

The inverse of companding is:

$$F^{-1}(r) = sgn(r)\begin{cases} \frac{|r|(1+ln(A))}{A}, & |r| < \frac{|r|_{max)}}{1+ln(A)} \\ \frac{exp(|r|(1+ln(A))-1)}{A}, & |r| \ge \frac{|r|_{max)}}{1+ln(A)} \end{cases} \quad (30)$$

#### 5.2.3. Rooting companding (RTC)

The rooting companding function is expressed by [46]:

$$C(x) = |x|^R * sgn(x) \quad (31)$$

Where $R$=0.1 to 0.9, which is related to the variations of the PAPR.

The de-companding function is known as:

$$C'(x) = |x|^{\frac{1}{R}} * sgn(x) \tag{32}$$

### 5.2.4. Cos (cos) companding

The representation of the cos function is as follows [38, 46]:

$$C(x) = sgn(x)\sqrt[y]{\alpha\left[1 - cos\left(-\frac{|x|}{\sigma}\right)\right]} \tag{33}$$

At the receiver, the de-companding is:

$$C'(x) = sgn(x)\left|-\sigma acos\left(1 - \frac{|x|^{\frac{2}{y}}}{\alpha}\right)\right| \tag{34}$$

$\alpha$ determines the average output signal power and $y$ varies between 0.1 and 1.

$$\alpha = \left(\frac{E\left[|x|^2\right]}{E\left[\sqrt[d]{\left[1-exp\left(-\frac{|x|}{\sigma}\right)\right]^2}\right]}\right)^{\frac{y}{2}} \tag{35}$$

### 5.2.5. Tangent rooting (tanhR) companding

Eq. (36) writes the tanhR companding [46, 47, 48]:

$$C(x) = tanh((|x| * k)^y) * sgn(x) \tag{36}$$

Where $k$ is a positive value that controls the level of companding applied to the envelope $x$ and $k$ varies between 5 and 25. The positive variable $y$ varies between 0.2 and 1. The inverse function companding is:

$$C'(y) = \left|\left(atanh\left(\frac{|x|}{k}\right)\right)^{\frac{1}{y}}\right| sgn(x) \tag{37}$$

### 5.2.6. Logarithmic rooting (logR) companding

The logR companding function is written as [39, 47]:

$$C(x) = log((|x| * k)^y + 1)sgn(x) \tag{38}$$

where $k$ is a positive value that represents the companding parameters and allows to control the companding level applied.

The definition of the inverse logR companding is:

$$C'(y) = \left|\left(exp\left(\frac{|x|}{k}\right) - 1\right)^{\frac{1}{y}}\right| sgn(x) \tag{39}$$

## 6. Combining companding and RCF techniques in MIMO FBMC/OQAM system

This considered scheme uses a serial combination of two techniques based on RCF and companding to further reduce the PAPR. Fig. 1 depicts the suggested block diagram. The complex signal *x(t)* is modulated, then transmitted to the IFFT block as an OQAM signal. In the time domain, the transformed FBMC signal passes via a clipping block and is then reconverted to the frequency domain for filtering. The last step is to retransform the signal into the time domain and compand it. This filtering and clipping process is repeated $I$ times to eliminate the reproduction of signal peaks or OOB distortion. The signal is subsequently sent through a transmission channel by 2x2 antennas. In the reception, we equalized the input signal by MMSE block and de-companded it, then performed the FFT phase and demodulated it to reproduce the original signal *x(t)*.

## 7. Simulation and result

This section discusses the PAPR and BER performance results of several hybridizations of the RCF technique with each companding technique, including A-Law, Mu-Law, tanhR, logR, cos and RTC. In the simulations, we use two antennas on transmit and receive parts with a Rayleigh channel and implementation of MMSE equalizer.

Also, this section presents the individual performances of several companding techniques in terms of PAPR and BER in the first step, then analyzes the performance of companding and RCF hybridizations in the second step. The parameters and variables utilized in the simulations are listed in Table 1 and Table 2.

Fig. 2 shows the PAPR versus the number of subcarriers in a MIMO-FBMC OQAM system and plots the numerical results at *CCDF*=$10^{-3}$. The PAPR improves as the number of subcarriers decreases. For $N$=128 sub-carriers, the lowest PAPR is achieved (17.80dB). At $N$=1024 subcarriers, the highest PAPR is generated (18.65dB).

In Fig. 3, we Illustrate the PAPRs of various companding techniques at *CCDF*= $10^{-3}$. The Mu-Law method has the best PAPR reduction performance,

Table 1. Simulation parameters

| Symbols | Parameters | Values |
|---|---|---|
| $N$ | Number of subcarriers | 128 |
| Phydyas | Filter | / |
| $K$ | Overlapping factor | 4 |
| $M$ | Data blocks | $10^5$ |
| OQAM | Modulation | 4OQAM |
| $CR$ | Clipping Ratio | 3 |
| $I$ | Number of RCF Iterations | 4 |

Table 2. List of techniques variables

| Techniques | variables | Values |
|---|---|---|
| Mu-Law | $Mu$ | 300 |
| A-Law | $A$ | 90 |
| RTC | $R$ | 0.6 |
| cos | $y$ | 0.6 |
| tanhR | $y$ | 0.7 |
| | $k$ | 10 |
| logR | $k$ | 10 |
| | $y$ | 0.62 |

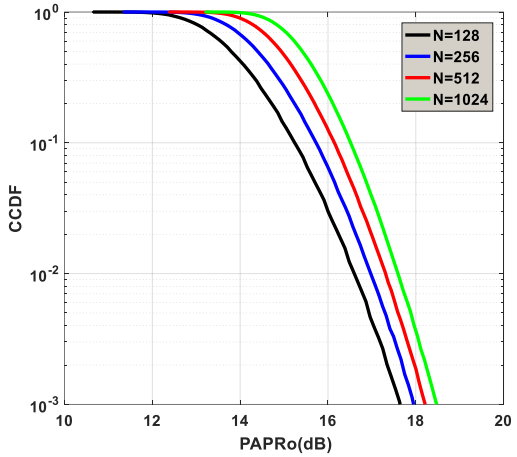


Figure. 2 PAPR of MIMO-FBMC OQAM with subcarriers $N$

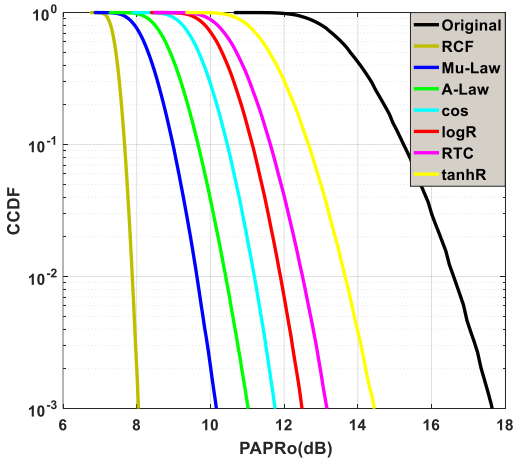


Figure. 3 PAPR of FBMC based on companding techniques

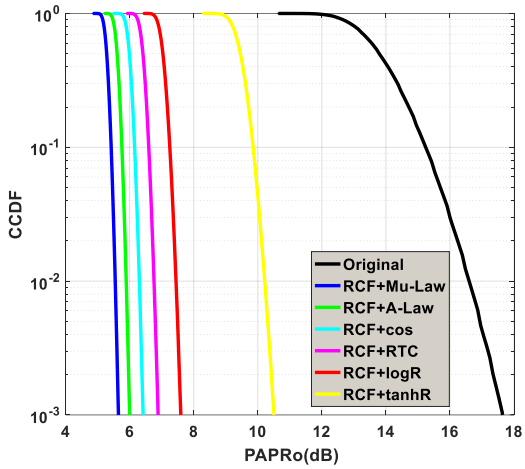


Figure. 4 PAPR of MIMO FBMC OQAM based on RCF with companding techniques

Table 2. PAPR reduction for various combinations

| Reduction techniques | PAPR without hybridization | PAPR with hybridization | Gap |
|---|---|---|---|
| Original | 17.8dB | / | / |
| Mu-Law | 10.1dB | 5.6dB | 4.5dB |
| A-Law | 11dB | 6dB | 5dB |
| cos | 11.8dB | 6.4dB | 5.4dB |
| logR | 12.5dB | 7.5dB | 5.0dB |
| RTC | 13dB | 6.8dB | 6.2dB |
| tanhR | 14.4dB | 10.5dB | 3.9dB |

followed by the A-Law with 10.10dB and 11dB, respectively. The latest methods, tanhR and RTC, have a PAPR reduction of 14.40dB and 13dB,respectively. Moreover, the RCF technique, with 8dB, significantly reduces the PAPR compared to all other companding techniques.

Fig. 4 compares the hybridizations of the RCF with companding techniques at $CCDF$=$10^{-3}$. The Mu-Law (5.6dB) presents the best hybridization in terms of PAPR reduction, while the A-Law indicates the second (6dB). The tanhR method (10.5dB) denotes the last hybridization, which is preceded by the logR (7.5dB).

As shown in Table 2, the hybridization scheme illustrates significant reduction in PAPR compared to the previous one in Fig. 3. RTC hybridization decreases by 6.2dB, followed by cos combination with PAPR reduction of 5.4dB. The last in the ranking presented by the tanhR combination reduces the PAPR by 3.9dB, preceded by 4.5dB for the Mu-Law version.

The BER of the MIMO FBMC/OQAM system is shown in Fig. 05 for various combinations of PAPR

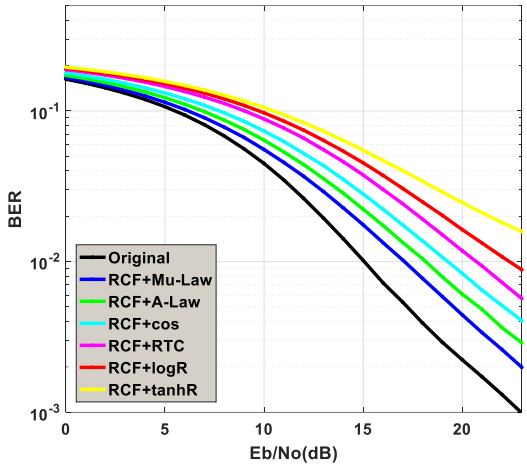


Figure. 5 BER performance of RCF and Companding techniques hybridization in MIMO FBMC OQAM scheme

reduction. Plots of BER show minimal variation between different hybridizations. The Mu-Law combination represents the best BER, followed by the A-Law and the worst is tanhR.

The RCF combined with Mu-Law offers the best PAPR reduction and BER performance, according to measurements supported by numerical results, followed by hybridization with the A-Law technique.

## 8. Conclusion

In this article, the PAPR reduction technique suggested was thoroughly studied. Separately, the RCF and companding methods reduce PAPR with less complexity. The combination of these techniques resulted in both significant PAPR reduction and good BER results. Knowing that the RCF and the Mu-Law hybridization produced the best results. The PAPR for the MIMO FBMC/OQAM system without a reduction method went from 17.8dB to 4.5dB with the suggested technique. Although the RCF efficiently reduces the PAPR, the Mu-Law technique compensates for the RCF's BER degradation to a large amount. In addition, this combination can be implemented in a future wireless scheme to reduce the PAPR of the FBMC system.

## Conflicts of interest

The authors declare no conflict of interest.

## Author contributions

Conceptualization, Ammar Boudjelkha; methodology, Ammar Boudjelkha and Abdellatif Khelil; software, Ammar Boudjelkha; validation, Ammar Boudjelkha, Abdellatif Khelil and Hocine Merah; formal analysis, Ammar Boudjelkha; investigation, Ammar Boudjelkha; resources, Ammar Boudjelkha; data curation, Ammar Boudjelkha; writing—original draft preparation, Ammar Boudjelkha; writing—review and editing, Ammar Boudjelkha; visualization, Ammar Boudjelkha; supervision, Abdellatif Khelil and Hocine Merah; project administration, Abdellatif Khelil. All authors read and approved the final manuscript

## References

[1] S. Jang, D. Na, and K. Choi, "Comprehensive performance comparison between OFDM-based and FBMC-based uplink systems", In: *Proc. of 2020 International Conference on Information Networking (ICOIN)*, Barcelona, Spain, pp. 288-292, 2020.

[2] B. A. Adoum, K. Zoukalne, M. S. Idriss, A. M. Ali, A. Moungache, and M. Y. Khayal, "A Comprehensive Survey of Candidate Waveforms for 5G, beyond 5G and 6G Wireless Communication Systems", *Open Journal of Applied Sciences*, Vol. 13, No. 1, pp. 136-161, 2023.

[3] X. Cheng, D. Liu, W. Shi, Y. Zhao, Y. Li, and D. Kong, "A novel conversion vector-based low-complexity SLM scheme for PAPR reduction in FBMC/OQAM systems", *IEEE Transactions on Broadcasting*, Vol. 66, No. 3, pp. 656-666, 2020.

[4] L. Li, L. Xue, X. Chen, and D. Yuan, "Partial transmit sequence based on discrete particle swarm optimization with threshold about PAPR reduction in FBMC/OQAM system", *IET Communications*, Vol. 16, No. 2, pp. 142-150, 2022.

[5] K. Tahkoubit, H. Shaiek, D. Roviras, S. Faci, and A. A. Pacha, "Generalized Iterative Dichotomy PAPR Reduction Method for Multicarrier Waveforms", *IEEE Access*, Vol. 9, pp. 114235-114245, 2021.

[6] Y. Lu, F. Hu, L. Jin, J. Liu, and G. Zhang, "Continuous unconstrained PSO-PTS strategy to maximize HPA energy efficiency for FBMC-OQAM systems", *IET Communications*, Vol. 17, No. 5, pp. 614-631, 2023.

[7] H. Merah, Y. Merrad, M. H. Habaebi, and M. Mesri, "A novel PTS-based PAPR reduction scheme for FBMC-OQAM system without extra bit transmission of SI", *International Journal of Electronics*, Vol. 108, No. 6, pp. 928-944, 2021.

[8] Z. Kollár and P. Horváth, "PAPR reduction of FBMC by clipping and its iterative

compensation", *Journal of Computer Networks and Communications*, 2012.

[9] M. K. Srivastava, M. K. Shukla, N. Srivastava, and A. K. Shankhwar, "A hybrid scheme for low PAPR in filter bank multi carrier modulation", *Wireless Personal Communications*, Vol. 113, No. 2, pp. 1009-1028, 2020.

[10] S. Senhadji, Y. M. Bendimerad, and F. T. Bendimerad, "New scheme for PAPR reduction in FBMC-OQAM systems based on combining TR and deep clipping techniques", *International Journal of Electrical & Computer Engineering*, Vol. 11, No. 3, pp. 2088-8708, 2021.

[11] V. Sundeepkumar and S. Anuradha, "Adaptive clipping-based active constellation extension for PAPR reduction of OFDM/OQAM signals", *Circuits, Systems, and Signal Processing*, Vol. 36, No. 7, pp. 3034-3046, 2017.

[12] G. M. Salama, H. F. Abdalla, A. A. Mohamed, E. S. Hassan, M. I. Dessouky, A. A. M. Khalaf, A. E. Emary, and A. S. Elsafrawey, "PAPR reduction technique for FBMC based visible light communication systems", *IET Communications*, Vol. 16, No. 15, pp. 1807-1814, 2022.

[13] J. Zhao, S. Ni, and Y. Gong, "Peak-to-average power ratio reduction of FBMC/OQAM signal using a joint optimization scheme", *IEEE Access*, Vol. 5, pp. 15810-15819, 2017.

[14] I. A. A. Shaheen, A. Zekry, F. Newagy, and R. Ibrahim, "Absolute exponential companding to reduced papr for fbmc/oqam", In: *Proc. of 2017 Palestinian International Conference on Information and Communication Technology (PICICT), IEEE*, Gaza City, pp. 60-65, 2017.

[15] I. A. Shaheen, A. Zekry, F. Newagy, and R. Ibrahim, "Modified square rooting companding technique to reduced PAPR for FBMC/OQAM", In: *Proc. of 2017 Palestinian International Conference on Information and Communication Technology (PICICT), IEEE*, Gaza City, pp. 66-70, 2017.

[16] S. Ramavath and U. C. Samal, "PAPR Reduction of FBMC Signals Based on Uniform and Linear PDF Companding Schemes", *arXiv preprint* arXiv:2108.03608, 2021.

[17] S. Ramavath and U. C. Samal, "Theoretical analysis of papr companding techniques for fbmc systems", *Wireless Personal Communications*, Vol. 118, No. 4, pp. 2965-2981, 2021.

[18] I. A. Shaheen, A. Zekry, F.Newagy, and R. Ibrahim, "Performance evaluation of PAPR reduction in FBMC system using nonlinear companding transform", *ICT Express*, Vol. 5, No. 1, pp. 41-46, 2019.

[19] A. Hasan, M. Zeeshan, M. A. Mumtaz, and M. W. Khan, "PAPR reduction of FBMC-OQAM using A-law and Mu-law companding", In: *Proc. of 2018 ELEKTRO*, Mikulov, Czech Republic, pp. 1-4, 2018.

[20] A. Mobin and A. Ahmad, "PAPR reduction of FBMC-OQAM systems using logarithmic rooting companding", In: *Proc. of 2021 Fourth International Conference on Electrical, Computer and Communication Technologies (ICECCT). IEEE*, Erode, India, pp. 1-6, 2021.

[21] I. A. Shaheen and A. Zekry, "Design New Companding Scheme to Reduced PAPR for FBMC/OQAM in 5G Communication", In: *Proc. of 2020 International Conference on Promising Electronic Technologies (ICPET)*, Jerusalem, Palestine, pp. 66-71, 2020.

[22] X. Li, D. Wang, Z. Li, W. Bai, X. Hu, and R. Fu, "A Hybrid TSLM and A-Law Companding Scheme for PAPR Reduction in FBMC-OQAM Systems", In: *Proc. of 2020 International Wireless Communications and Mobile Computing (IWCMC)*, Limassol, Cyprus, pp. 1077-1081, 2020.

[23] R. Gopal and S. K. Patra, "Combining tone injection and companding techniques for PAPR reduction of FBMC-OQAM system", In: *Proc. of 2015 Global Conference on Communication Technologies (GCCT)*, Thuckalay, India, pp. 709-713, 2015.

[24] H. Hesham and T. Ismail, "Hybrid NOMA-based ACO-FBMC/OQAM for next-generation indoor optical wireless communications using LiFi technology", *Optical and Quantum Electronics*, Vol. 54, No. 3, p. 201, 2022.

[25] V. S. Kumar, "Joint iterative filtering and companding parameter optimization for PAPR reduction of OFDM/OQAM signal", *AEU-International Journal of Electronics and Communications*. Vol. 124, p. 153365, 2020.

[26] M. Masarra, K. Hassan, M. Zwingelstein, and I. Dayoub, "FBMC-OQAM for frequency-selective mmWave hybrid MIMO systems", In: *Proc. of 2022 IEEE wireless communications and networking conference (WCNC)*, Austin, TX, USA, pp. 1593-1598, 2022.

[27] K. Choi, "Alamouti coding for DFT spreading-based low PAPR FBMC", *IEEE Transactions on Wireless Communications*, Vol.18, No. 2, pp. 926-941, 2018.

[28] I. A. Shaheen, A. Zekry, F. Newagy, R. Ibrahim, "Proposed new schemes to reduce PAPR for

STBC MIMO FBMC systems", *Simulation*, Vol.6, No. 9, 2017.

[29] H. Wang, L. Xu, X. Wang, and S. Taheri, "Preamble design with interference cancellation for channel estimation in MIMO-FBMC/OQAM systems", *IEEE Access*, Vol. 6, pp. 44072-44081, 2018.

[30] V. S. Kumar, "PAPR Reduction Method for MIMO-OFDM/OQAM System Based on SFBC Structure", In: *Proc. of Soft Computing and Signal Processing: Proceedings of 3rd ICSCSP 2020*, Springer Singapore, Vol. 1, pp. 607-615, 2021.

[31] H. Merah, M. Mesri, K. Tahkoubit, and L. Talbd, "PAPR reduction in MIMO (2× 2)-FBMC-OQAM systems using attenuating QAM symbols", In: *Proc. of 2019 6th International Conference on Image and Signal Processing and their Applications (ISPA), IEEE*, Mostaganem, Algeria, pp. 1-5, 2019.

[32] I. A. Shaheen, A. Zekry, F. Newagy, and R. Ibrahim, "PAPR reduction using combination of SAS preprocessed and WHT precoding for MIMO system of FBMC/OQAM transceiver", *International Journal of Engineering & Technology*, Vol. 7, No. 4, pp. 3803-3809, 2018.

[33] D. Kong, J. Li, K. Luo, and T. Jiang, "Reducing pilot overhead: channel estimation with symbol repetition in MIMO-FBMC systems", *IEEE Transactions on Communications*, Vol. 68, No 12, pp. 7634-7646, 2020.

[34] H. Wang, W. Du, X. Wang, G. Yu, and L. Xu, "Channel estimation performance analysis of FBMC/OQAM systems with bayesian approach for 5G-enabled IoT applications", *Wireless Communications and Mobile Computing*, 2020.

[35] S. Taheri, M. Ghoraishi, and P. Xiao, "Overhead reduced preamble-based channel estimation for MIMO-FBMC systems", In: *Proc. of 2015 international wireless communications and mobile computing conference (IWCMC)*, Dubrovnik, Croatia, pp. 1435-1439, 2015.

[36] D. Kong, P. Liu, Q. Wang, J. Li, X. Li, and X. Cheng, "Preamble-based MMSE channel estimation with low pilot overhead in MIMO-FBMC systems", *IEEE Access*, Vol. 8, pp. 148926-148934, 2020.

[37] P. Jirajaracheep, T. Mata, and P. Boonsrimuang, "PAPR reduction in FBMC-OQAM systems using trellis-based D-SLM with ABC algorithm", In: *Proc. of 2020 17th International Conference on Electrical Engineering/Electronics, Computer, Telecommunications and Information Technology (ECTI-CON)*, Phuket, Thailand, pp. 506-509, 2020.

[38] A. Agarwal, and R. Sharma, "Review of different PAPR reduction techniques in FBMC-OQAM system", *In Internet of Things and Big Data Applications*, Springer, Cham, pp. 183-191, 2020.

[39] S. Kaur, L. Kansal, G. S. Gaba, F. Alraddady, and S. K. Arora, "Impact of Hybrid PAPR Reduction Techniques on FBMC for 5G Applications", *International Journal on Smart Sensing and Intelligent Systems*, Vol. 13, No. 1, p. 1, 2020.

[40] A. Kumar and H. Rathore, "Reduction of PAPR in FBMC system using different reduction techniques", *Journal of Optical Communications*, Vol. 42, No. 2, pp. 303-309, 2021.

[41] X. Yi, B. Wang, W. Zhao, and M. Jin, "Hybrid PAPR Reduction Algorithm Using Low Complexity Dispersive Selective Mapping with Clipping and Filtering for FBMC/OQAM", In: *Proc. of 2019 Eleventh International Conference on Ubiquitous and Future Networks (ICUFN). IEEE*, Zagreb, Croatia, pp. 532-537, 2019.

[42] S. K. Deng and M. C. Lin, "Recursive clipping and filtering with bounded distortion for PAPR reduction", *IEEE Transactions on communications*, Vol. 55, No. 1, pp. 227-230, 2007.

[43] M. R. A. Yassin, H. Abdallah, H. Issa, and S. A. Chahine, "Universal Filtered Multi-Carrier Peak to Average Power Ratio Reduction", *J. Commun.*, Vol. 14, No. 3, pp. 243-248, 2019.

[44] R. Patra, A. Mahapatro, H. B. Mishra, P. Singh, and S. Panda, "PAPR and CCDF Analysis of Superimposed Training Sequence-based MIMO-FBMC OQAM Systems", In: *Proc. of TENCON 2019-2019 IEEE Region 10 Conference (TENCON), IEEE*, Kochi, India, pp. 1489-1493, 2019.

[45] V. S. Kumar, J. T. Kumar, S. Merugu, and K. Srinivas, "PAPR Reduction Scheme for OFDM/OQAM Signals Using Novel Phase Sequence", *Data Engineering and Communication Technology*, Springer, Singapore, pp. 211-219, 2021.

[46] S. Nokaiee and M. AlKhawlani, "New Hybrid Schemes for PAPR Reduction in OFDM Systems", *Journal of Science and Technology*, Vol. 23, No. 1, pp. 17-38, 2018.

[47] S. M. Farid, H. Elbadawy, and K. Shehata, "Energy Efficiency Improvement in Mobile Communication System by Reducing the

PAPR", *Journal of Physics: Conference Series. IOP Publishing*, Vol. 1447, No. 1, p. 012043, 2020.

[48] M. S. A. E. Galil, N. F. Soliman, M. I. Abdalla, M. A. Elaskily, and F. E. A. E. Samie, "TanhR nonlinear companding scheme for UWA systems", *International Journal of Electronics Letters*, Vol. 9, No. 4, pp. 517-523, 2021.